Influence of high-pressure homogenization on structural properties and enzymatic hydrolysis of milk proteins

D. Carullo[1], F. Donsì[1], G. Ferrari[1,2*]

[1]Department of Industrial Engineering, University of Salerno, Via Giovanni Paolo II, 132 – 84084 Fisciano (SA), Italy

[2]ProdAl Scarl – University of Salerno, Via Giovanni Paolo II, 132 – 84084 Fisciano (SA), Italy

*Corresponding author: Prof. Eng. Giovanna Ferrari
Tel.: +39089964134
E-mail address: gferrari@unisa.it (G. Ferrari)

Abstract

This study investigated the effects of HPH processing parameters on the conformational structure of bovine serum albumin (BSA) and whey protein isolate (WPI).

BSA and WPI dispersions (1% w/v in phosphate buffer, pH = 7.5) were treated in a bench-scale HPH unit at different pressures (100, 150, 200 MPa) and number of passes (1, 2, 3, 5). The modifications of proteins' primary structure (carbonyl groups), secondary structure (α-helix, β-sheet, turn), tertiary and quaternary structure (free -SH groups) were analyzed together with their particle size distribution (PSD). HPH-assisted hydrolysis with trypsin and α-chymotrypsin was performed (200 MPa, 1 pass). Hydrolysis degree and molecular weight distribution of peptides were determined and compared with those of untreated protein dispersions.

HPH treatments did not affect proteins' primary structure while slight modifications of secondary structure were detected. Interestingly, free - SH groups in BSA increased with increasing the pressure due to partial unfolding, while decreased in WPI, possibly due to disaggregation and compaction of native WPI aggregates. HPH pre-treatment allowed enhancing BSA hydrolysis reaction rate, while the compaction of WPI aggregates caused a reduced hydrolysis extent. In conclusion, HPH caused an appreciable modification of protein conformation and affected the degree of enzymatic hydrolysis.

Keywords – High-pressure homogenization (HPH), bovine serum albumin (BSA), whey protein isolate (WPI), denaturing gel electrophoresis (SDS-PAGE), enzymatic hydrolysis.

1. Introduction

In the last decades, food and biotechnological industries have focused on different nonthermal technologies (pulsed electric fields, pulsed light, high hydrostatic pressure, high-pressure homogenization) as a platform for the development of new food-processing and preservation methods, characterized by minimal impacts on both nutritional and organoleptic properties of foods.

Within this frame, an emerging field is represented by the change or modulation of the techno-functional properties of proteins, promoting and expanding their applicability, at industrial scale, for the formulation/development of novel foods (De Maria, Ferrari, & Maresca, 2016; Wu et al., 2019). Proteins are key food ingredients, due to their ability to form/stabilize emulsions or foams, to bind specific compounds, to increase solution viscosity, or to improve aggregation/gelation phenomena (Bouaouina, Desrumaux, Loisel, & Legrand, 2006). These properties can be tuned by applying thermal or mechanical stresses, which may eventually cause a greater exposure of free sulfhydryl groups upon molecular unfolding, with a subsequent increase in hydrophobic interactions (Dissanayake & Vasiljevic, 2009; Maresca et al., 2017, Siddique, Maresca, Pataro, & Ferrari, 2016). In particular, high-pressure homogenization (HPH) represents a promising tool to significantly modify both the conformation and the main functional properties of several food proteins or enzymes (Aguilar, Cristianini, & Sato, 2018; Bouaouina et al., 2006; Liu et al., 2011; Liu & Kuo, 2016; Luo et al., 2010; Pereda, Ferragut, Buffa, Guamis, & Trujillo, 2008; Shen & Tang, 2012; Sørensen et al., 2014; Yu, Wu, Cha, Qin, & Du, 2018). Moreover, HPH technology offers the advantage of easy scale-up to great production volumes, as shown for different applications of potential industrial interest (Ali et al., 2018; Dong et al., 2011; Donsì, Annunziata, & Ferrari, 2013).

HPH is a purely fluid-mechanical process, based on the forced passage of a solution or a suspension, under high pressure (typically, in the range 50-300 MPa), through a specifically designed micrometric disruption valve (Carullo et al., 2018). During HPH processing, the pressure energy accumulated in the fluid is instantaneously released as turbulent kinetic energy, causing intense fluid-mechanical stresses, and frictional heat, which generates high temperature local hot spots (Coccaro, Ferrari, & Donsì, 2018). The combination of these phenomena results not only in the efficient disruption of suspended particles or plant/microbial cells, but also in protein structural alteration (Carullo et al., 2018; Donsì, Ferrari, Lenza, & Maresca, 2009; Jurić, Ferrari, Velikov, & Donsì, 2019; Panozzo et al., 2014; Saricaouglu, Gul, Besir, & Atalar, 2018; Wang et al., 2019).

HPH treatments have been described to cause reversible or irreversible alteration of the tertiary and quaternary structure of proteins, by affecting inter/intramolecular hydrophobic and electrostatic interactions (Keerati-u-rai & Corredig, 2009; Sørensen et al., 2014; Yuan, Ren, Zhao, Luo, & Gu, 2012). However, to date, controversial results were reported about the effect of HPH on protein secondary structure (Bouaouina et al., 2006; Maresca et al., 2017; Subirade, Loupil, Allain, & Paquin, 1998; Wu et al., 2019).

More recently, the recovery and subsequent functionalization via HPH processing of proteins derived from cheese whey has attracted considerable interest for the possibility to simplify waste management (Mollea, Marmo, & Bosco, 2013), as well as to provide pharmaceutical, chemical and food industries with more advanced products (Liu et al., 2011; Maresca et al., 2017). For instance, Liu et al. (2011) demonstrated that the application of HPH treatments between 40 and 160 MPa significantly improved the foam formation/stabilization properties of whey proteins concentrate (WPC) in comparison with untreated samples. This behavior was attributed to the increase in protein flexibility and mobility under pressure, hence enabling a more efficient entrapment of air bubbles at the gas/liquid interface. Similarly, Bouaouina et al. (2006) found that the increase in hydrophobic interactions generated during HPH (P = 50 – 300 MPa) positively affected whey proteins foamability over control dispersions. Remarkably, no effects of HPH pressure on whey proteins solubility have been reported (Dissanayake & Vasiljevic, 2009).

It may be inferred that the HPH induced unfolding/aggregation phenomena could potentially influence whey proteins susceptibility to enzymatic hydrolysis, thus supporting their potential exploitation in several industrial sectors (De Maria, Ferrari, & Maresca, 2017).

To the best of our knowledge, only the work of Blayo, Vidcoq, Lazennec & Dumay (2016) has previously shown that HPH treatment (300 MPa) accelerated the reaction rates of enzymatic hydrolysis of whey proteins. The authors attributed this behavior to partial unfolding, which increased the accessibility of trypsin to the target hydrolysis sites. Maresca et al. (2017) reported the successful application of HPH treatments to promote structural changes of bovine serum albumin (BSA), as well

as to positively affect its techno-functional properties (e.g. foamability). However, the authors did not perform any investigation on the impact of HPH treatments on BSA hydrolysis.

Despite β-Lg is the most abundant protein in whey (Verheul, Roefs, Mellema, & de Kruif, 1998), whey proteins' properties and functionality do not depend only on its conformational changes, but also on the combined properties of all WP components (β-Lg, α-Lactoalbumin, BSA, amongst others), as well as on their mutual interactions under pressure (Ali et al., 2018).

The present work assessed the HPH treatment as a physical manipulation method for enabling the control of the structural properties and the rate of enzymatic hydrolysis of proteins. To this purpose, a protein mixture (whey proteins) and a pure protein (BSA), naturally contained in whey in a small amount (≈5% w/w), were chosen as separated test systems, to evidence the dependence of the effect of HPH processing on protein characteristics. Trypsin and α-chymotrypsin were selected as highly effective enzymes for both whey proteins and bovine serum albumin degradation reactions.

2. Materials and Methods

2.1.Preparation of protein dispersion and chemicals

In this work, two different protein sources were used: powdered bovine serum albumin (BSA, purity > 98%, CAS No. 9048-46-8), which was purchased from Sigma-Aldrich (Milan, Italy), and lyophilized whey protein isolate (WPI, UltraWhey 90 instant), derived from sweet cheese whey, which was purchased from Volac International Ltd. (Orwell, UK). According to the manufacturer's specifications, the weight composition of the WPI powder was as follows: 90% proteins, 1.0% fat, 2.0% lactose, 2.2% ash, and 4.0% moisture. The protein fraction included β-lactoglobulin (43–48%), α-lactalbumin (14–18%), bovine serum albumin (1–2%), immunoglobulin G (1–3%), and lactoferrin (< 1%). Both raw materials were stored under refrigerated conditions (T = 4 °C) until their usage. All chemicals and enzymes used in this study were purchased from Sigma Aldrich (Milan, Italy) unless otherwise specified. MilliQ water was used to dilute samples and prepare all reagents and buffers.

Before HPH processing, both BSA and WPI powders were dissolved at a constant concentration (1% w/v) in a sodium phosphate buffer (50 mmol/L, pH = 7.5) and kept under gentle stirring in an ice-water bath until complete solubilization. The controlled value of pH, which was measured using a pH-meter (S400 Seven Excellence, Mettler Toledo International Inc.), was necessary to minimize the effect of aggregation due to the increased electrostatic repulsions among polypeptides in dispersions, thus allowing to isolate the single effect exerted by HPH processing (Maresca et al., 2017).

2.2.High-pressure homogenization treatments

HPH treatments were performed in an in-house developed laboratory scale high-pressure homogenizer, as described elsewhere (Carullo et al., 2018). BSA and WPI samples were forced to pass through an orifice valve (model WS1973, Maximator JET GmbH, Schweinfurt, Germany) with interchangeable orifices in a size range 80 – 150 μm, upon pressurization using an air-driven Haskel pump (model DXHF-683, EGAR S.r.l., Milan, Italy). Changing the orifice size enabled to control pressure drop between 100 and 200 MPa, while the volumetric flow rate of the suspension was 155 mL/min. To prevent excessive temperature increases due to frictional heating, the dispersions were cooled at 5 °C in two tube-in-tube exchangers, one located between the pump and the homogenization valve, and one immediately downstream of the valve. In addition, the feeding tank was thermostated with a cooling jacket, also set at 5°C.

In the first set of experiments, BSA and WPI dispersions were separately subjected to HPH processing at variable pressure (P = 100 – 200 MPa) and number of passes (n_P = 1, 2, 3, 5). At the end of each treatment, samples were collected in plastic tubes and immediately placed in ice until analyzed. Untreated samples (controls) were also collected and used as a reference for further characterizations. The second set of experiments investigated the effect of an HPH treatment, carried out at constant processing conditions (P = 200 MPa, n_P = 1), as a pre-treatment stage before enzymatic hydrolysis, which was initiated by adding either trypsin (1000-2000 BAEE units/mg solid) or α-chymotrypsin

147 (≥40 units/mg protein) to the protein samples, immediately after the HPH treatment. Hydrolysis
148 reactions were performed at a constant enzyme to substrate ratio (1:10 w/w) into an incubator shaker
149 (ω = 160 rpm) at 37 °C, corresponding to the activation temperature of the proteolytic enzymes
150 utilized. Aliquots of 1 mL of untreated and HPH pre-treated protein dispersions were withdrawn at
151 10, 20, 30, 45, and 60 min after the start of the enzymatic hydrolysis. The reaction was stopped by
152 heating samples at 100 °C for at least 5 min and subsequently stored at 4 °C before determining the
153 hydrolysis degree.
154

155 *2.3. Analytical measurements of BSA and WPI dispersions*

156 *2.3.1. Carbonyl groups*

157 Carbonyl groups content of untreated and HPH treated BSA and WPI samples was determined
158 according to the method reported in Levine et al. (1990), with some modifications as described in a
159 previous paper (Siddique et al., 2016). An aliquot of a protein sample, corresponding to 2 mg of
160 protein, was incubated with 10 mmol/L 2, 4- Dinitrophenylhydrazin (DNPH) in 2 mol/L HCl (1 mL),
161 for 30 min at room temperature (25 °C). Afterward, 1 mL of a 10% (w/v) trichloroacetic acid solution
162 was used to precipitate proteins, which were recovered by centrifugation at 6500×g for 5 min (ALC
163 PK130, Cologno Monzese (MI), Italy). Protein pellets were washed three times with 1 mL of
164 ethanol/ethyl acetate 50:50 (v/v) to remove residual unreacted molecules of DNPH and subsequently
165 dissolved in 1 mL of 6 mol/L urea (pH = 2.3). The concentration of carbonyl groups was determined
166 by spectrophotometry at 370 nm (V-650, Jasco Inc. Easton, MD, USA) using an extinction coefficient
167 of 2.2×10^4 L mol^{-1} cm^{-1} (Scheidegger, Pecora, Radici, & Kivatinitz, 2010).
168

169 *2.3.2. Free -SH groups*

170 Determination of free -SH groups of both untreated and HPH treated protein samples was carried out
171 according to the method developed by Ellman (1959), with slight modifications. The protein

dispersions were diluted to a final concentration of 2 g/L with a 50 mmol/L Tris-HCl buffer (pH = 7.0) in 15 mL plastic tubes. Afterward, 2.75 mL of diluted protein was mixed with 0.25 mL of a 5,5'-dithiobis 2-nitrobenzoic acid (DTNB) solution (1 g/L) in 50 mmol/L Tris-HCl buffer. Absorbance was measured by spectrophotometry at 412 nm against a blank (2.75 mL of 50 mmol/L Tris-HCl buffer + 0.25 mL of DTNB reactant), 30 min after the start of the chemical reaction. The concentration of free -SH groups was calculated as reported in Siddique et al. (2016), with the results expressed as μmol free -SH groups/g protein.

2.3.3. Particle size distribution (PSD)

The particle size distribution of untreated and HPH treated protein dispersions was measured by dynamic light scattering (DLS) using an HPPS instrument (Malvern instrument Ltd., Malvern, U.K.). Measurements of DLS were carried out applying backscatter detection NIBS (Non- Invasive Back-Scatter) technology at 173°. For the measurements, 1.5 mL of undiluted BSA or WPI samples was poured into disposable sizing cuvettes. The temperature of the cell was maintained at 25 ± 0.5 °C during measurements. The detection range of particle size was from 0.3 nm to 10 μm and the PSD curves were obtained as the averages of 15 runs per repetition from the extrapolation of the translational diffusion coefficient (Dt) according to the Stokes-Einstein equation.

2.3.4. Aggregation index and turbidity

UV–Vis spectra of all samples (untreated, HPH-treated) were evaluated by spectrophotometry and their shape was plotted as a function of the investigated range of wavelengths (λ = 200 – 800 nm). The spectra were corrected for the absorbance of sodium phosphate buffer (pH = 7.5). Aggregation in BSA and WPI was assessed using an aggregation index (A.I.), which was calculated utilizing the formulae reported by Katayama et al. (2005).

196 Instead, the turbidity of BSA and WPI samples without further dilutions was measured at room
197 temperature and reported as the value of the absorbance at 420 nm, according to the work of Ju &
198 Kilara (1998).

199

200 *2.3.5. FT-IR measurements*

201 Attenuated total reflection infrared (ATR FT-IR) spectra of untreated and HPH treated BSA or WPI
202 dispersions (P = 200 MPa, n_P = 1) were measured according to the protocol described by Siddique et
203 al. (2016) by using an FTIR-4100 series spectrophotometer (Jasco Europe Srl, Italy).
204 The spectra were collected at a resolution of 2 cm^{-1} in the Amide I region (1700 - 1600 cm^{-1}) in the
205 double-sided, forward-backward mode and resulted from an average of 64 scans. The spectra of
206 protein dispersions were corrected by subtracting the background noise originating from the air,
207 moisture, and coating materials on reflecting mirrors along the IR radiation path. Nine repetitions
208 from each sample were used for each spectra measurement. The resulting averaged spectra were
209 smoothed with an eleven-point under adaptive-smoothing function to remove the eventual noises and
210 then baseline modification was applied.

211

212 *2.3.6. Hydrolysis degree by OPA reaction*

213 The determination of the hydrolysis degree of untreated at HPH pre-treated samples (P = 200 MPa,
214 n_P = 1) was made through the measurement of the o-phthaldialdehyde (OPA) reaction, according to
215 the method described by Nielsen, Petersen & Dambmann (2001). Briefly, OPA reagent was prepared
216 by dissolving sodium tetraborate decahydrate, sodium dodecyl sulfate (SDS), o-phthaldialdehyde
217 97% (OPA) and dithiothreitol 99% (DTT) in a deionized water solution. A serine solution (0.1 g/L)
218 in deionized water was used as standard. For each measurement, 3 mL of OPA reagent was added to
219 400 μL of deionized water (blank), serine solution (standard), or sample. The degree of hydrolysis

(DH%) was measured by spectrophotometry at 340 nm after 2 min of reaction by using the formula reported by Hardt, van der Goot & Boom (2013). All measurements were carried out at ambient temperature.

2.3.7. Reducing SDS-PAGE analysis

SDS-PAGE electrophoresis was carried out under reducing conditions as described by O'Loughlin et al. (2012), with slight modifications. A TV100Y twin-plate mini-gel unit equipped with an Apelex power supply unit (APELEX-Massy, France) was used. Samples of native proteins (BSA, WPI), pretreated proteins by HPH and HPH-assisted hydrolyzed proteins were diluted in a Tris-HCl buffer (0.125 mol/L, pH = 6.8) containing SDS (2% w/w), glycerol (10% w/w), bromophenol blue (0.02% w/w) and β-mercaptoethanol (5% w/w) as reducing agent. The acrylamide for the separating gel (12% w/v) was prepared in 1.5 mol/L Tris-HCl buffer (pH = 8.8), with a stacking gel (6% w/v) prepared in 0.5 mol/L Tris-HCl buffer (pH = 6.8). Before pouring the gels, 50 µL of ammonium persulfate solution (10% w/v) and 5 µL of N, N, N', N'-tetra methylethylenediamine (TEMED) were added to both the separating and stacking gel solutions. 5 µL of all samples were loaded into the prepared gels and run at constant voltage (100 V) for 1h. To monitor the electrophoretic separation process, 5 µL of a peqGOLD pre-stained Protein Marker (10 – 260 kDa) were also added to the gels. Gels were then stained with a staining solution (0.1% Coomassie Brilliant Blue R 250, 10% acetic acid, 20% isopropanol) overnight. Subsequently, a de-staining solution (30% methanol, 10% acetic acid) was used until the background became clear.

2.4.Statistical analysis

All treatments and analyses were performed in triplicates, with the mean values and standard deviations (SD) of the experimental data subsequently calculated. Statistically significant differences

244 ($p \leq 0.05$) among the averages, both in terms of structural properties and associated hydrolysis
245 degrees, were evaluated using a one-way analysis of variance (ANOVA) and Tukey's test ($p \leq 0.05$).
246 Statistical analyses were carried out using IBM SPSS Statistics 20 software (SPSS Inc., Chicago,
247 USA).

248

249 **3. Results and Discussion**

250 *3.1. Effects of HPH treatments on protein primary structure: carbonyl groups analysis*

251 The measurement of changes in protein carbonyl groups indirectly provides an indication of the
252 damages occurring in protein primary structure upon the application of different physicochemical
253 treatments (Siddique et al., 2016). Protein carbonyl groups are mainly generated by oxidative
254 reactions, which may influence either sensitive side chains or protein backbone, leading to its
255 fragmentation (Levine et al., 1990).
256 Table 1 reports the content of carbonyl groups, expressed in nmol/mg protein, for untreated (control)
257 and HPH-treated samples of BSA and WPI, as a function of HPH pressure and number of passes (P
258 = 100 – 200 MPa, n_P = 1 – 5). Regardless of the severity of the HPH treatment, no significant ($p >$
259 0.05) alterations of the primary structure of BSA and WPI were achieved, in comparison with control
260 samples. Coherently, SDS-PAGE analyses did not evidence any reduction of the average molecular
261 weight of HPH-treated BSA or WPI (data not shown). Thus, under the conditions investigated in this
262 work, it can be concluded that HPH does not induce modifications of the protein's primary structure.
263 This is in agreement with previous findings on HPH-treated β-Lg (Chen et al., 2019) or trypsin (Liu
264 et al., 2010). Moreover, Chen et al. (2012) highlighted that changes in protein primary structure can
265 be induced only at significantly higher pressures (8 GPa).

266

3.2. Effects of HPH treatments on proteins unfolding and aggregation: free -SH groups, PSD, aggregation index and turbidity

The mean concentrations of free -SH groups in untreated and HPH treated BSA and WPI samples at variable pressure and number of passes are reported in Table 2. The change in free -SH groups represents a reliable and macroscopic indicator of the degree of unfolding/denaturation phenomena occurring in proteins upon the application of physical stresses (Liu & Kuo, 2016; Siddique et al., 2016). When proteins are in their native state, the majority of -SH groups are hidden inside poorly accessible regions of the polypeptide chain, thus hardly coming in contact with Ellman's reagent (DTNB). However, when the unmasking of free thiol groups occurs due to unfolding, the accessibility of DTNB to reaction sites is dramatically improved (De Maria et al., 2016; Siddique et al., 2016).

The data of Table 2 suggest that, independently of the protein tested, a pressure of 100 MPa did not significantly affect ($p > 0.05$) the tertiary and quaternary structures, as shown by the concentrations of free -SH groups, which are similar to those of native samples. However, when the pressurization intensity was increased to 150 - 200 MPa, significant differences were observed for BSA and WPI samples. In particular, BSA underwent a significant increase ($p \leq 0.05$) of free -SH groups over untreated samples, which may be ascribed either to partial unfolding (Maresca et al., 2017) or to intramolecular disulfide bonds cleavage (Yu et al., 2018). The highest concentration of thiol groups was detected in BSA dispersions treated at 200 MPa for one pass. At the highest pressure level (200 MPa), the increased number of passes negatively affected free -SH groups concentration, which was reduced by about 10% from 1 to 5 passes.

In agreement, Maresca et al. (2017) showed that increasing the number of passes at 200 MPa promoted the formation of disulfide bridges, which reduced both the concentration of free -SH groups and foaming capacity of BSA dispersions.

Instead, in the case of WPI dispersions, HPH treatments at $P \geq 150$ MPa caused a slight but significant reduction ($p \leq 0.05$) in free -SH groups in comparison with untreated samples. This may be due to

292 the excessive energy transferred to the polypeptide chains, which might have caused compaction of
293 WPI aggregates and, consequently, further masking of the free -SH groups.
294 These results are in good agreement with the findings of Shen & Tang (2012), who observed a
295 reduction of free -SH groups in soy protein isolates treated at 120 MPa, which was attributed to the
296 formation of new disulfide bonds through SH/SS intra- or intermolecular reactions.
297 The interpretation of the data of Table 2 can be supported by the PSD curves of untreated and HPH-
298 treated samples at 200 MPa for $n_P = 1 – 5$, reported in Figure 1 for BSA (a) and WPI (b), respectively.
299 The application of HPH treatments at 100 MPa did not induce any significant change in PSD,
300 independently of the type of protein considered (data not shown).
301 Untreated BSA samples showed a monomodal size distribution curve, with the maximum at 8.72 nm,
302 which is compatible with the size of BSA monomers (66 kDa), as previously reported by Blayo et al.
303 (2016). Remarkably, regardless of the number of passes, PSD curves of HPH-treated BSA dispersions
304 exhibited a bimodal distribution, with a second peak in the range between 200 – 5500 nm, which
305 indicates the formation of aggregates, similarly to what reported by Maresca et al. (2017). This
306 behavior could be explained by the occurrence of protein unfolding, which promotes the increase of
307 intermolecular interactions and, subsequently, the formation of aggregates. The increased values of
308 the aggregation index and turbidity of HPH-treated BSA samples at 200 MPa, observed in Table 3,
309 confirm the results of PSD measurements. The formation of BSA aggregates upon HPH processing
310 at 200 MPa is also confirmed by the results of Figure S1a of the Supplementary Material. Specifically,
311 the addition of a denaturing agent, such as SDS, to HPH-treated BSA dispersions caused the almost
312 complete breakage of the aggregates, generating a PSD curve very similar to that of the untreated
313 samples.
314 In contrast, untreated WPI samples (Figure 1b) showed a bimodal distribution, characterized by a
315 first small peak at around 6 nm and a second bigger peak at around 300 nm. When HPH treatments
316 were carried out at 200 MPa, regardless of the number of passes, a slight shift of PSD curves towards
317 smaller sizes was detected, in agreement with literature data (Bouaouina et al., 2006; Liu et al. 2011).

318 Liu et al. (2011) postulated that the reduction of WPI mean particle size was a consequence of the
319 disaggregation and further reorganization of proteins in more stable and compacted structures, due to
320 the intense mechanical stresses of homogenization. These observations are supported by the
321 significant reduction in free -SH groups, as well as the slightly lower values of the aggregation index,
322 reported respectively in Tables 2 and 3.
323 Blayo et al. (2016) reported that WPI dispersions, subjected to HPH treatment at 250 MPa and 300
324 MPa, underwent unfolding/aggregation phenomena, which caused the shift of PSD curves of native
325 samples towards larger sizes. Therefore, it could be speculated that the unfolding of WPI is triggered
326 at a pressure level comprised between 200 MPa and 250 MPa. However, further investigation at
327 pressure levels higher than those applied in this work is needed to confirm this hypothesis.
328
329 *3.3.Effect of HPH treatments on the main protein secondary structures: α-helix, β-sheets, turn*
330 *components*
331 Fourier transform infrared spectroscopy (FT-IR) enabled to assess any qualitative variation of the
332 protein secondary structure induced by HPH treatment (P = 200 MPa; n_P = 1) of BSA and WPI
333 dispersions, through the comparison with the untreated sample (Figure 2).
334 The wavelength range 1700 – 1600 cm^{-1} (Amide I) can be related to the stretching vibrations of the
335 C = O bonds of the amide groups (De Maria et al., 2016), thus it is generally used to predict the
336 behavior of the secondary structure components of a polypeptide chain. In particular, spectra from
337 both untreated BSA (Figure 2a) and WPI samples (Figure 2b) are dominated by four characteristic
338 bands, at 1636 cm^{-1} (β-sheet intramolecular), 1651 cm^{-1} (α-helix), 1667 cm^{-1} (turn structures) and
339 1691 cm^{-1} (β-sheet intermolecular), according to the assignment by Barth (2007). In Figure 2, the
340 highest absorption peaks can be observed for both protein dispersions at 1636 cm^{-1}, indicating that
341 the secondary structure of native BSA and WPI samples is predominantly characterized by
342 intramolecular β-sheets.

343 Figure 2a highlights that a single HPH pass at 200 MPa only slightly affected the BSA secondary
344 structure, with a very small increase of intramolecular β-sheets and α-helix components over the
345 initial spectrum (controls). Partially in contrast with these results, Maresca et al. (2017) observed a
346 significant alteration of BSA secondary structure after the application of 1 HPH pass, independently
347 on the pressure level (P = 100 – 200 MPa). These discrepancies could be due to the different protein
348 concentration, the type of HPH equipment, and the analytical method utilized.
349 Data from Figure 2b show that significant differences are detected between untreated and HPH-
350 treated WPI dispersions, where an increase in the peaks associated to α-helix and intramolecular β-
351 sheet structures is accompanied by a slight reduction in the peaks corresponding to turn (1667 cm^{-1})
352 and β-sheet intermolecular (1691 cm^{-1}) structures. The analyzed WPI dispersion is a protein mixture,
353 and, therefore, the observed changes in secondary structures can not be associated with the changes
354 of individual proteins. However, the data still provide some important insights on the effect of HPH
355 treatment, which appears to be important especially for the disruption of protein aggregates,
356 coherently with the interpretation given of the data reported in Figure 1b. In can be hypothesized that
357 the observed changes are due to the high susceptibility of β-Lg, which is the most abundant
358 component of whey proteins, to pressure-induced variation of secondary structures. Nevertheless, this
359 hypothesis, which is in agreement with the significant increase in α-helix structures reported for
360 HPH-treated β-Lg samples at 160 MPa (Chen et al., 2019), needs to be validated by specific
361 experiments carried out on individual proteins.
362

363 *3.4. Effect of HPH treatments on protein susceptibility to enzymatic attack: hydrolysis degree and*
364 *peptides molecular weight distribution by SDS-PAGE*

365 The occurrence of new conformational states upon HPH processing in protein structures via
366 unfolding/aggregation phenomena suggests that HPH treatments could influence also proteins
367 enzymatic hydrolysis reactions.

368 The selected pressure level (P = 200 MPa) and number of passes (n_P = 1) for HPH pre-treatments
369 before enzymatic hydrolysis derives from the observation that the proteins tested in this work showed
370 opposite behaviors in terms of the effect on free -SH groups, which were maximized in the case of
371 BSA and minimized in the case of WPI, in comparison with native control samples.
372 Despite the proteolytic enzymes tested in this work (trypsin, α-chymotrypsin) have similar tertiary
373 structure and catalytic mechanism, they differ in substrate specificity. In particular, trypsin is reported
374 to hydrolyze peptide bonds in which the carboxyl groups are present on lysine and arginine residues,
375 while α-chymotrypsin is reported to cleave preferably peptide bonds on the C-terminal side of
376 phenylalanine, tyrosine, tryptophan, and leucine (De Maria et al., 2017).
377 Hydrolysis kinetics for untreated and HPH pre-treated samples of BSA and WPI are reported in
378 Figures 3 and 4, respectively. Only in the case of tryptic hydrolysis of BSA, the effect of enzyme
379 addition before or after the HPH treatment on yields and rates of hydrolysis has been compared to the
380 data obtained from conventional hydrolysis at ambient pressure.
381 Figures 3 and 4 clearly indicate that, independently of the protein, the hydrolysis extent increased
382 with the reaction time, with the maximum values of DH% detected after 60 min. However, the trends
383 of the hydrolysis reaction observed were very similar for both proteolytic enzymes, even though
384 higher DH% values were detected when using α-chymotrypsin (Figures 3b-4b). This can be explained
385 considering the higher substrate specificity of this enzyme, as already observed for high hydrostatic
386 pressure-assisted enzymatic hydrolysis of BSA (De Maria et al., 2017).
387 The HPH-induced unfolding of BSA protein significantly ($p \leq 0.05$) improved its susceptibility to
388 trypsin and chymotrypsin attack, thus accelerating the rate of reaction, with the hydrolysis degree
389 reaching the maximum values of 8.89% and 11.22% after 10 and 60 minutes, respectively (Figure 3).
390 Interestingly, when trypsin was added to BSA dispersions before HPH processing, comparable or
391 lower DH% values than control samples were obtained (Figure 3a). This can be explained considering
392 that the initial temperature of the dispersion was 5 °C, which is significantly lower than the optimal

393 temperature for hydrolytic enzyme activity of 37 °C. Moreover, it could be hypothesized that the
394 HPH process induced a slight enzyme inactivation. These observations are in good agreement with
395 the findings of Liu et al. (2010), who demonstrated that at a temperature between 25 °C and 35 °C
396 the activity of trypsin was significantly reduced after an HPH treatment at 120 MPa.
397 In contrast, HPH processing did not cause an increase in hydrolysis reaction yields and rates of WPI
398 dispersions, regardless of the enzyme (Figure 4). These results are consistent with the observed
399 reduction in free -SH groups (Table 2) and compaction of the structure of proteins (Figure 1b), thus
400 being less prone to proteolytic attack. Previously, Blayo et al. (2016) demonstrated that the
401 application of an HPH treatment at 300 MPa was necessary to significantly increase whey protein
402 hydrolysis by trypsin, because of enhanced enzyme accessibility to reaction sites upon protein
403 unfolding.
404 Data of Figures 3 and 4 are also confirmed by SDS-PAGE profiles of hydrolysates obtained from
405 HPH-treated BSA and WPI dispersions, for both investigated enzymes (Figures 5 and 6). The patterns
406 of native BSA and WPI, as well as of a protein marker, were also reported to identify the molecular
407 weight of the peptides produced. After 10 min of hydrolysis by trypsin, the content of native BSA,
408 which showed a major characteristic band between 50 and 70 kDa, was reduced and smaller peptides
409 formed, whose more intense bands are found at 50, 25, 18 and 12 kDa (Figure 5a). Similar profiles
410 were observed when using α-chymotrypsin (Figure 5b), except for the presence of additional bands
411 at high MW (100 – 260 kDa), which might be due to the aggregation of very small peptides (<10
412 kDa) produced during hydrolysis. Additionally, as the reaction time was increased, a slight
413 brightening of hydrolysates characteristic bands was observed, thus confirming the increasing trends
414 of DH% of Figure 3b.
415 Native WPI samples (Figure 6) clearly showed two main bands, respectively corresponding to β-
416 Lactoglobulin (15 kDa) and α-Lactoalbumin (between 10 and 15 kDa), together with a smaller
417 amount of BSA (between 50 and 70 kDa). The results of Figure 6 highlight a greater susceptibility of

418 α-Lactoalbumin to hydrolysis by both trypsin and α-chymotrypsin, which was degraded already after
419 10 min of reaction. On the contrary, in agreement with the findings of Kristo et al. (2012), β-Lg
420 required longer reaction times to be hydrolyzed, with a complete degradation detected only after 45
421 min of hydrolysis by α-chymotrypsin. Further studies on the characterization of the hydrolysates are
422 necessary to better elucidate the mechanistic effects of HPH on protein enzymatic hydrolysis.
423
424 **4. Conclusions**
425 In this work, the effects of HPH treatments applied at different pressure levels (P = 100 – 200 MPa)
426 and number of passes (n_P = 1 – 5) on conformational modification of BSA and WPI dispersions, as
427 well as on their susceptibility to enzymatic attack, were investigated.
428 Results demonstrated that a slight variation in protein secondary structure occurred for one HPH pass
429 at 200 MPa. However, such structural modifications were more marked in WPI rather than in BSA,
430 with an increase in α-helix and β-sheet intramolecular components over native samples.
431 Moreover, while HPH triggered unfolding/aggregation of BSA dispersions in the range 150 - 200
432 MPa, thus inducing a greater protein susceptibility to enzymatic attack, an opposite trend was detected
433 for WPI, which then negatively affected the performances of the hydrolysis reaction.
434 Additional studies are required to better elucidate the role and the interactions between the mechanical
435 stresses occurring during HPH treatments and the initial characteristics of the protein source, to
436 develop a technological platform to physically manipulate protein conformation, techno-functional
437 properties and susceptibility to enzymatic hydrolysis, thus expanding their range of application in
438 different industrial sectors.
439
440 **Acknowledgments**
441 Daniele Carullo is indebted to the University of Salerno (Dept. of Industrial Engineering) for having
442 provided funds for his post-doctoral scholarship.

443 **References**

444 Aguilar, J.G.d.S. Cristianini, M., & Sato, H.H. (2018). Modification of enzymes by use of high-
445 pressure homogenization. *Food Research International*, 109, 120–125.

446 Ali, A., Le Potier, I., Huang, N., Rosilio, V., Cheron, M., Faivre, V., Turbica, I., Agnelya, F., &
447 Mekhloufi, G. (2018). Effect of high pressure homogenization on the structure and the interfacial and
448 emulsifying properties of β-lactoglobulin. *International Journal of Pharmaceutics*, 537, 111–121.

449 Barth, A. (2007). Infrared spectroscopy of proteins. *Biochimica et Biophysica Acta*, 1767, 1073–1101.

450 Blayo, C., Vidcoq, O., Lazennec, F., & Dumay, E. (2016). Effects of high pressure processing
451 (hydrostatic high pressure and ultra-high pressure homogenisation) on whey protein native state and
452 susceptibility to tryptic hydrolysis at atmospheric pressure. *Food Research International*, 79, 40–53.

453 Bouaouina, H., Desrumaux, A., Loisel, C., & Legrand, J. (2006). Functional properties of whey
454 proteins as affected by dynamic high-pressure treatment. *International Dairy Journal*, 16, 275–284.

455 Carullo, D., Abera, B.D., Casazza, A.A., Donsì, F., Perego, P., Ferrari, G., & Pataro, G. (2018). Effect
456 of pulsed electric fields and high pressure homogenization on the aqueous extraction of intracellular
457 compounds from the microalgae Chlorella vulgaris. *Algal Research*, 31, 60-69.

458 Chen, W.-Q., Heymann, G., Kursula, P., Rosner, M., Hengstschlager, M., Huppertz, H., & Lubec, G.
459 (2012). Effects of Gigapascal Level Pressure on Protein Structure and Function. The Journal of
460 Physical Chemistry, 116, 1100-1110.

461 Chen, H., Hong, Q., Zhong, J., Zhou, L., Liu, W., Luo, S., & Liu, C. (2019). The enhancement of
462 gastrointestinal digestibility of b-LG by dynamic high-pressure microfluidization to reduce its
463 antigenicity. *International Journal of Food Science and Technology*, 54, 1677–1683.

464 Coccaro, N., Ferrari, G., Donsì, F. (2018). Understanding the break-up phenomena in an orifice-valve
465 high pressure homogenizer using spherical bacterial cells (Lactococcus lactis) as a model disruption
466 indicator. *Journal of Food Engineering*, 236, 60–71.

467 De Maria, S., Ferrari, G., & Maresca, P. (2016). Effects of high hydrostatic pressure on the
468 conformational structure and the functional properties of bovine serum albumin. *Innovative Food*
469 *Science and Emerging Technologies*, 33, 67–75.

470 De Maria, S., Ferrari, G., & Maresca, P. (2017). Effect of high hydrostatic pressure on the enzymatic
471 hydrolysis of bovine serum albumin. *Journal of the Science of Food and Agriculture*, 97, 3151–3158.

472 Dissanayake, M., & Vasiljevic, T. (2009). Functional properties of whey proteins affected by heat
473 treatment and hydrodynamic high-pressure shearing. *Journal of Dairy Science*, 92, 1387-1397.

474 Dong, X., Zhao, M., Shi, J., Yang, B., Li, J., Luo, D., Jiang, G., & Jiang, Y. (2011). Effects of
475 combined high-pressure homogenization and enzymatic treatment on extraction yield, hydrolysis and
476 function properties of peanut proteins. *Innovative Food Science and Emerging Technologies*, 12,
477 478–483.

478 Donsì, F., Ferrari, G., Lenza, E, & Maresca, P. (2009). Main factors regulating microbial inactivation
479 by high-pressure homogenization: Operating parameters and scale of operation. *Chemical*
480 *Engineering Science*, 64, 520-532.

481 Donsì, F., Annunziata, M., & Ferrari, G. (2013). Microbial inactivation by high pressure
482 homogenization: Effect of the disruption valve geometry. *Journal of Food Engineering*, 115, 362–
483 370.

484 Ellman, G. L. (1959). Tissue sulfhydryl groups. *Archives of Biochemistry and Biophysics*, 82, 70–77.

485 Hardt, N.A., van der Goot, A.J., Boom, R.M. (2013). Influence of high solid concentrations on
486 enzymatic wheat gluten hydrolysis and resulting functional properties. *Cereal Science*, 57, 531-536.

Ju, Z. Y., & Kilara, A. (1998). Aggregation induced by calcium chloride and subsequent thermal gelation of whey protein isolate. *Journal of Dairy Science*, 81, 925–931.

Jurić, S., Ferrari, G., Velikov, K. P., Donsì, F. (2019). High-pressure homogenization treatment to recover bioactive compounds from tomato peels. *Journal of Food Engineering*, 262, 170-180.

Katayama, D. S., Nayar, R., Chou, D. K., Campos, J., Cooper, J., Vander Velde, D. G., Vilarete, L., Liu, C.P., & Manning, M. C. (2005). Solution behavior of a novel type 1 interferon-tau. *Journal of Pharmaceutical Sciences*, 94, 2703–2715.

Keerati-u-rai, M., & Corredig, M. (2009). Effect of Dynamic High Pressure Homogenization on the Aggregation State of Soy Protein. *Journal of Agricultural and Food Chemistry*, 57, 3556-3562.

Kristo, E., Hazizaj, A., & Corredig, M. (2012). Structural Changes Imposed on Whey Proteins by UV Irradiation in a Continuous UV Light Reactor. *Journal of Agricultural and Food Chemistry*, 60, 6204-6209.

Levine, R. L., Garland, D., Oliver, C. N., Amici, A., Climent, I., Lenz, A. G., Ahn, B.W., Shaltiel, S., & Stadtman, E. R. (1990). Determination of carbonyl content in oxidatively modified proteins. *Methods in Enzymology*, 186, 464–478.

Liu, W., Zhang, Z.Q., Liu, C.-M., Xie, M.-Y., Tu, Z.-C., Liu, J.-H., & Liang, R.-H. (2010). The effect of dynamic high-pressure microfluidization on the activity, stability and conformation of trypsin. *Food Chemistry*, 123, 616-621.

Liu, C.-M., Zhong, J.-Z., Liu, W., Tu, Z.-C., Wan, J., Cai, X.-F., & Song, X.-Y. (2011). Relationship between Functional Properties and Aggregation Changes of Whey Protein Induced by High Pressure Microfluidization. *Journal of Food Science*, 76, E341-E347.

Liu, H.H., & Kuo, M.-I. (2016). Ultra high pressure homogenization effect on the proteins in soy flour. *Food Hydrocolloids*, 52, 741-748.

510 Luo, D., Zhao, Q., Zhao, M., Yang, B., Long, X., Ren, J., & Zhao, H. (2010). Effects of limited
511 proteolysis and high-pressure homogenisation on structural and functional characteristics of glycinin.
512 *Food Chemistry*, 122, 25–30.

513 Maresca, P., Ferrari, G., de Castro Leite Júnior, B.R., Zanphorlin, L.M., Ribeiro, L.R., Murakami,
514 M.T., & Cristianini, M. (2017). Effect of dynamic high pressure on functional and structural
515 properties of bovine serum albumin. *Food Research International*, 99, 748–754.

516 Mollea, C., Marmo, L., & Bosco, F. (2013). Valorisation of Cheese Whey, a By-Product from the
517 Dairy Industry. In I. M. (Eds.), *Food Industry* (pp. 549-588). InTECH Publisher.

518 Nielsen, P.M., Petersen, D., & Dambmann, C. (2001). Improved method for determining food protein
519 degree of hydrolysis. *Food and Chemical Toxicology*, 66, 642-646.

520 O 'Loughlin, I. B., Murray, B.A., Kelly, P.M., Fitz Gerald, R.J., & Brodkorb, A. (2012). Enzymatic
521 hydrolysis of heat-induced aggregates of whey protein isolate. *Journal of Agricultural and Food*
522 *Chemistry*, 60, 4895-4904.

523 Panozzo, A., Manzocco, L., Calligaris, S., Bartolomeoli, I., Maifreni, M., Lippe, G., & Nicoli, M.C.
524 (2014). Effect of high pressure homogenisation on microbial inactivation, protein structure and
525 functionality of egg white. *Food Research International*, 62, 718–725.

526 Pereda, J., Ferragut, V., Buffa, M., Guamis, B., & Trujillo, A.J. (2008). Proteolysis of ultra-high
527 pressure homogenised treated milk during refrigerated storage. *Food Chemistry*, 111, 696–702.

528 Saricaoglu, F.T., Gul, O., Besirt, A., & Atalar, I. (2018). Effect of high pressure homogenization
529 (HPH) on functional and rheological properties of hazelnut meal proteins obtained from hazelnut oil
530 industry by-products. *Journal of Food Engineering*, 233, 98-108.

531 Scheidegger, D., Pecora, R. P., Radici, P. M., & Kivatinitz, S. C. (2010). Protein oxidative changes
532 in whole and skim milk after ultraviolet or fluorescent light exposure. *Journal of Dairy Science*, 93,
533 5101–5109.

534 Shen, L., & Tang, C.-H. (2012). Microfluidization as a potential technique to modify surface
535 properties of soy protein isolate. *Food Research International*, 48, 108–118.

536 Siddique, M.A.B., Maresca, P., Pataro, G., & Ferrari, G. (2016). Effect of pulsed light treatment on
537 structural and functional properties of whey protein isolate. *Food Research International*, 87, 189-
538 196.

539 Sørensen, H., Mortensen, K., Sørland, G.H., Larsen, F.H., Paulsson, M., & Ipsen, R. (2014). Dynamic
540 ultra-high pressure homogenisation of milk casein concentrates: Influence of casein content.
541 *Innovative Food Science and Emerging Technologies*, 26, 143–152.

542 Subirade, M., Loupil, F., Allain, A.-F., & Paquin, P. (1998). Effect of Dynamic High Pressure on the
543 Secondary Structure of b-Lactoglobulin and on its Conformational Properties as Determined by
544 Fourier Transform Infrared Spectroscopy. *Internationa Dairy Journal*, 8, 135-140.

545 Verheul, M., Roefs, S. P. F. M., Mellema, J., & de Kruif, K. G. (1998). Power law behavior of
546 structural properties of protein gels. *Langmuir*, 14, 2263–2268.

547 Wang, C., Ma, Y., Liu, B., Kang, Z., Geng, S., Wang, J., Wei, L., & Ma, H. (2019). Effects of dynamic
548 ultra-high pressure homogenization on the structure and functional properties of casein. *International*
549 *Journal of Agricultural & Biological Engineering*, 12, 229-234.

550 Wu, F., Shi, X., Zou, H., Zhang, T., Dong, X., Zhu, R., & Yu, C. (2019). Effects of high-pressure
551 homogenization on physicochemical, rheological and emulsifying properties of myofibrillar protein.
552 *Journal of Food Engineering*, 263, 272–279.

553 Yu, C., Wu, F., Cha, Y., Qin, Y., & Du, M. (2018). Effects of High-Pressure Homogenization at
554 Different Pressures on Structure and Functional Properties of Oyster Protein Isolates. *International*
555 *Journal of Food Engineering*, 14, DOI: 10.1515/ijfe-2018-0009.

556 Yuan, B., Ren, J., Zhao, M., Luo, D., & Gu, L. (2012). Effects of limited enzymatic hydrolysis with
557 pepsin and high-pressure homogenization on the functional properties of soybean protein isolate.
558 *LWT - Food Science and Technology*, 46, 453-459.

559 **Figure captions**

560

561 **Figure 1.** Particle size distribution (PSD) intensity averaged curves, obtained by dynamic light
562 scattering measurements, of untreated (●) and HPH treated BSA (a) or WPI (b) dispersions at 200
563 MPa and 1 pass (○), 2 passes (▼), 3 passes (△), or 5 passes (■).

564 **Figure 2.** Fourier transform infrared spectra of untreated (■) and HPH treated (■) BSA (a) and
565 WPI (b) samples (200 MPa, 1 pass). Each spectrum is plotted as a function of the wavenumber (cm^{-1}).

566 **Figure 3.** Kinetics of enzymatic hydrolysis of untreated (■) and HPH (■) pre-treated (200 MPa, 1
567 pass) BSA samples in the presence of trypsin (a) and α-chymotrypsin (b) enzymes. Different letters
568 above the bars indicate statistical differences among the samples ($p \leq 0.05$). Only in the case of tryptic
569 hydrolysis (a), reaction kinetics for samples added with the enzyme before HPH processing (■) are
570 also reported.

571 **Figure 4.** Kinetics of enzymatic hydrolysis of untreated (■) and HPH (■) pre-treated (200 MPa, 1
572 pass) WPI samples in the presence of trypsin (a) and α-chymotrypsin (b) enzymes. Different letters
573 above the bars indicate statistical differences among the samples ($p \leq 0.05$).

574 **Figure 5.** Reducing SDS-PAGE patterns of native and HPH-assisted hydrolyzed BSA (200 MPa, 1
575 pass) by trypsin (a) or α-chymotrypsin (b), as a function of the hydrolysis reaction time (t = 10 – 60
576 min).

577 **Figure 6.** Reducing SDS-PAGE patterns of native and HPH-assisted hydrolyzed WPI (200 MPa, 1
578 pass) by trypsin (a) or α-chymotrypsin (b), as a function of the hydrolysis reaction time (t = 10 – 60
579 min).

580 **Table 1** Concentration of carbonyl groups (nmol/mg protein) from untreated (control, 0.1 MPa) and
581 HPH treated BSA and WPI dispersions, as a function of the homogenization pressure (P, MPa) and
582 the number of passes (n_P) applied. Different superscript lowercase letters in the same column indicate
583 significant differences among mean values ($p<0.05$).

		Carbonyl groups [nmol C=O/mg protein]	
P [MPa]	n_P	BSA	WPI
0	0	1.60 ± 0.27^a	1.00 ± 0.15^a
100	1	1.47 ± 0.37^a	0.87 ± 0.09^a
	2	1.50 ± 0.30^a	0.87 ± 0.03^a
	3	1.63 ± 0.49^a	0.91 ± 0.04^a
	5	1.55 ± 0.30^a	0.91 ± 0.06^a
150	1	1.92 ± 0.17^a	0.89 ± 0.06^a
	2	1.94 ± 0.09^a	0.86 ± 0.10^a
	3	1.95 ± 0.36^a	0.90 ± 0.07^a
	5	1.91 ± 0.20^a	0.94 ± 0.08^a
200	1	1.52 ± 0.09^a	1.08 ± 0.02^a
	2	1.49 ± 0.02^a	1.07 ± 0.24^a
	3	1.44 ± 0.10^a	1.11 ± 0.08^a
	5	1.42 ± 0.07^a	1.07 ± 0.27^a

584
585
586
587
588
589

590 **Table 2** Concentration of free sulfhydryl groups (μmol/g protein) from untreated (control, 0.1 MPa)
591 and HPH treated BSA and WPI dispersions, as a function of the homogenization pressure (P, MPa)
592 and the number of passes (n_P) applied. Different superscript lowercase letters in the same column
593 indicate significant differences among mean values ($p<0.05$).

		Free sulfhydryl groups [μmol -SH/g protein]	
P [MPa]	n_P	BSA	WPI
0	0	8.19 ± 0.37^{a}	3.64 ± 0.22^{c}
100	1	8.12 ± 0.14^{a}	3.33 ± 0.13^{bc}
	2	8.06 ± 0.03^{a}	3.44 ± 0.16^{c}
	3	8.03 ± 0.19^{a}	3.38 ± 0.13^{c}
	5	8.09 ± 0.15^{a}	3.38 ± 0.12^{c}
150	1	9.05 ± 0.25^{c}	3.21 ± 0.09^{abc}
	2	9.43 ± 0.19^{c}	3.22 ± 0.11^{abc}
	3	9.50 ± 0.61^{c}	3.15 ± 0.10^{ab}
	5	9.27 ± 0.19^{c}	3.15 ± 0.23^{ab}
200	1	10.29 ± 0.19^{d}	2.97 ± 0.13^{a}
	2	9.35 ± 0.27^{c}	2.95 ± 0.11^{a}
	3	8.91 ± 0.40^{b}	2.89 ± 0.10^{a}
	5	9.22 ± 0.11^{c}	2.89 ± 0.17^{a}

594
595
596
597
598
599

Table 3 Values of aggregation indexes (A.I) and turbidity from untreated (control, 0.1 MPa) and HPH treated BSA and WPI dispersions, as a function of the homogenization pressure (P, MPa) and the number of passes (n_P) applied. Different superscript lowercase letters in the same column indicate significant differences among mean values ($p<0.05$).

		Aggregation index (A.I.)		Turbidity (A_{420nm})	
P [MPa]	n_P	BSA	WPI	BSA	WPI
0	0	2.65 ± 0.43^{a}	1.95 ± 0.11^{a}	0.016 ± 0.004^{a}	0.032 ± 0.004^{a}
100	1	2.97 ± 1.24^{ab}	2.25 ± 0.19^{a}	0.020 ± 0.010^{ab}	0.033 ± 0.018^{a}
	2	2.72 ± 0.72^{a}	2.06 ± 0.15^{a}	0.025 ± 0.005^{ab}	0.032 ± 0.001^{a}
	3	2.92 ± 0.89^{ab}	1.91 ± 0.20^{a}	0.025 ± 0.004^{ab}	0.032 ± 0.004^{a}
	5	2.85 ± 1.17^{ab}	1.86 ± 0.10^{a}	0.030 ± 0.12^{ab}	0.032 ± 0.003^{a}
150	1	$4.89 \pm 1.31a^{ab}$	2.21 ± 0.17^{a}	0.084 ± 0.032^{bc}	0.038 ± 0.012^{a}
	2	4.17 ± 0.36^{ab}	2.02 ± 0.18^{a}	0.068 ± 0.012^{abc}	0.036 ± 0.005^{a}
	3	5.14 ± 1.63^{ab}	1.95 ± 0.20^{a}	0.088 ± 0.040^{c}	0.036 ± 0.004^{a}
	5	4.18 ± 0.33^{ab}	1.81 ± 0.13^{a}	0.064 ± 0.004^{abc}	0.036 ± 0.007^{a}
200	1	6.25 ± 1.90^{b}	1.91 ± 0.48^{a}	0.088 ± 0.036^{c}	0.032 ± 0.014^{a}
	2	4.50 ± 1.02^{ab}	1.78 ± 0.19^{a}	0.048 ± 0.020^{abc}	0.030 ± 0.004^{a}
	3	4.72 ± 1.61^{ab}	1.83 ± 0.21^{a}	0.056 ± 0.036^{abc}	0.034 ± 0.006^{a}
	5	4.31 ± 1.16^{ab}	1.77 ± 0.20^{a}	0.040 ± 0.016^{abc}	0.033 ± 0.008^{a}

Supplementary Material

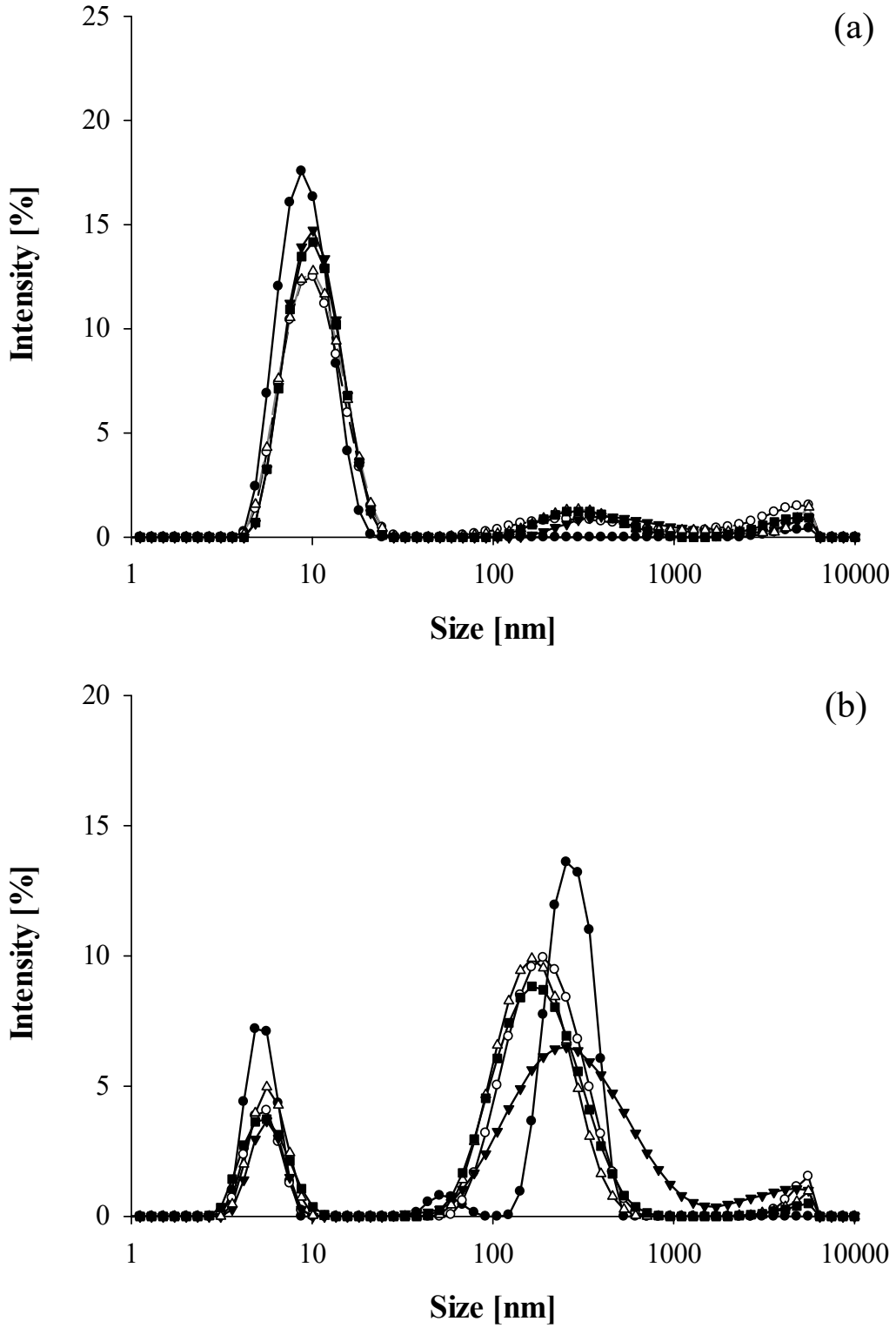

Figure S1. Particle size distribution (PSD) intensity averaged curves, obtained by dynamic light scattering measurements, of untreated (black circle) and HPH treated BSA (a) or WPI (b) dispersions at 200 MPa and 1 pass (white circle), 2 passes (black triangle), 3 passes (white triangle) or 5 passes (black square), in presence of SDS agent.

Figure 1

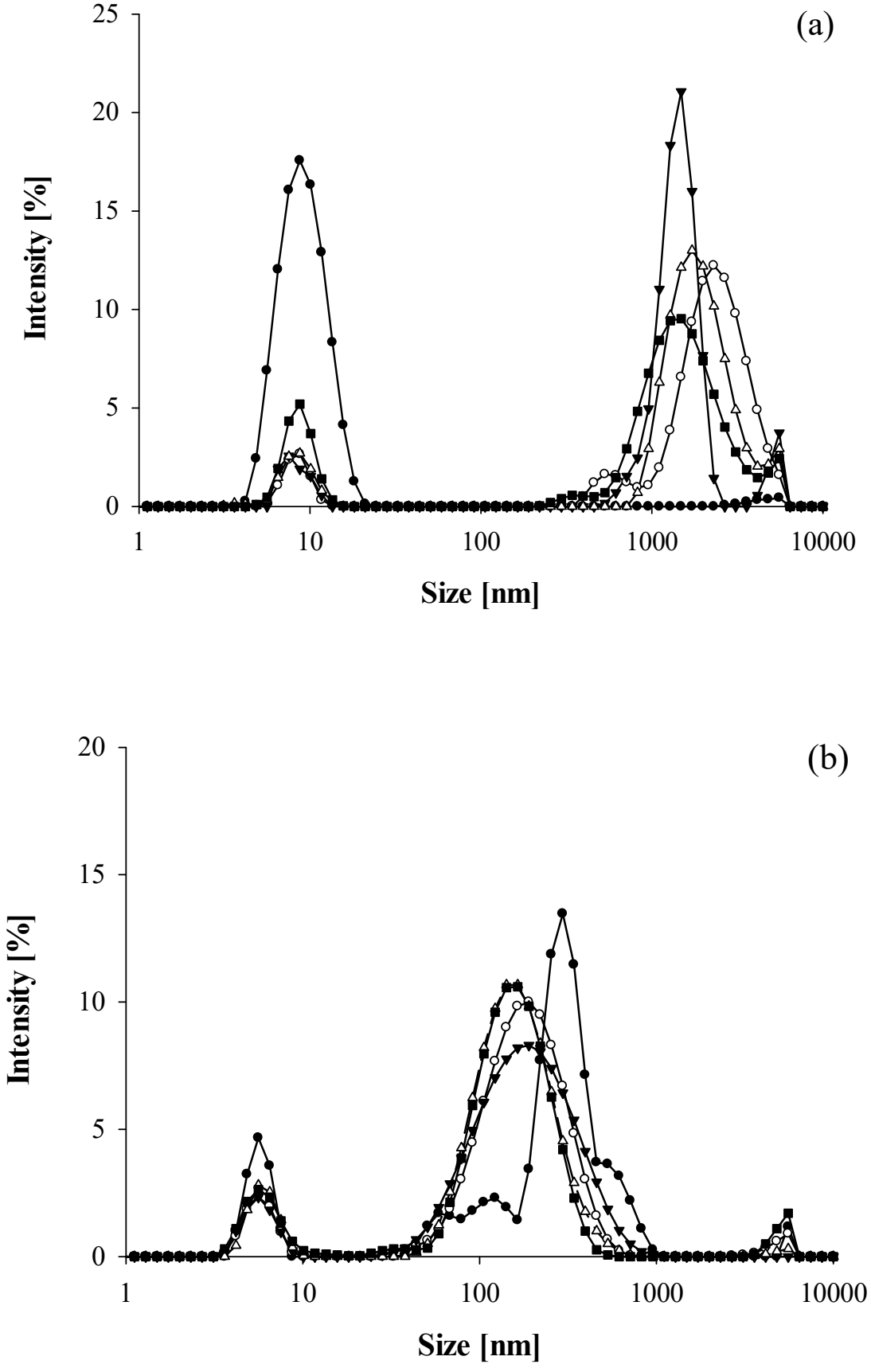
(a)
Intensity [%]
25
20
15
10
5
0
1
10
100
1000
10000
Size [nm]
(b)
Intensity [%]
20
15
10
5
0
1
10
100
1000
10000
Size [nm]

Figure 2

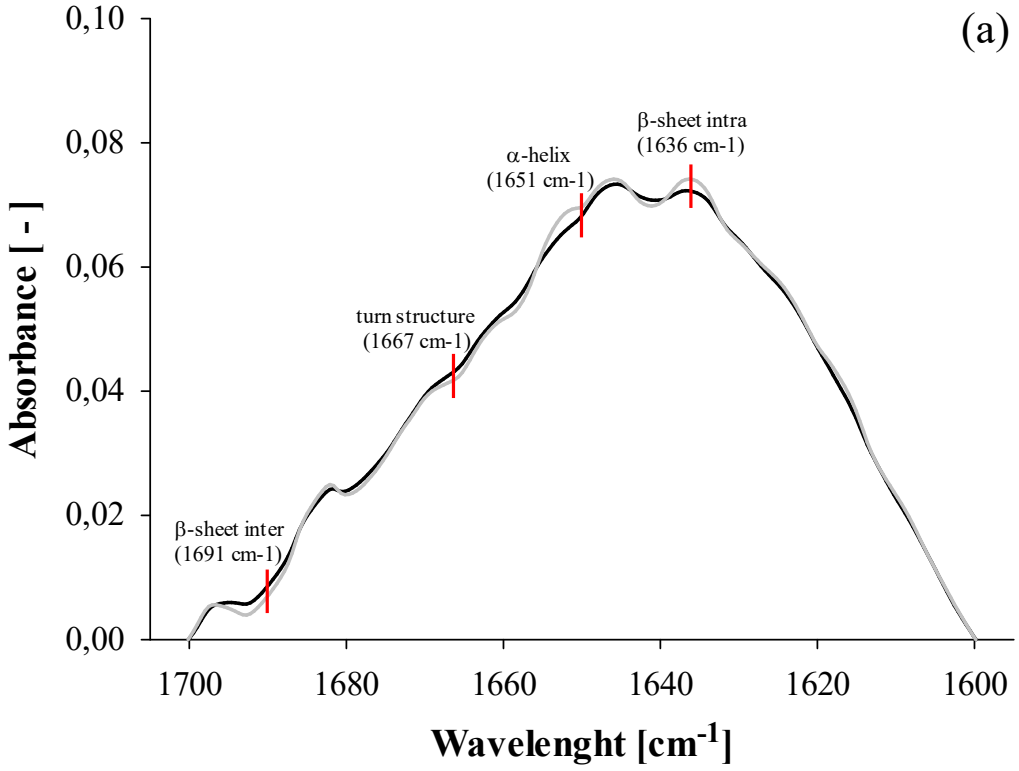
(a)
0,10
0,08
0,06
0,04
0,02
0,00
Absorbance [-]
β-sheet intra
(1636 cm-1)
α-helix
(1651 cm-1)
turn structure
(1667 cm-1)
β-sheet inter
(1691 cm-1)
1700
1680
1660
1640
1620
1600
Wavelenght [cm-1]

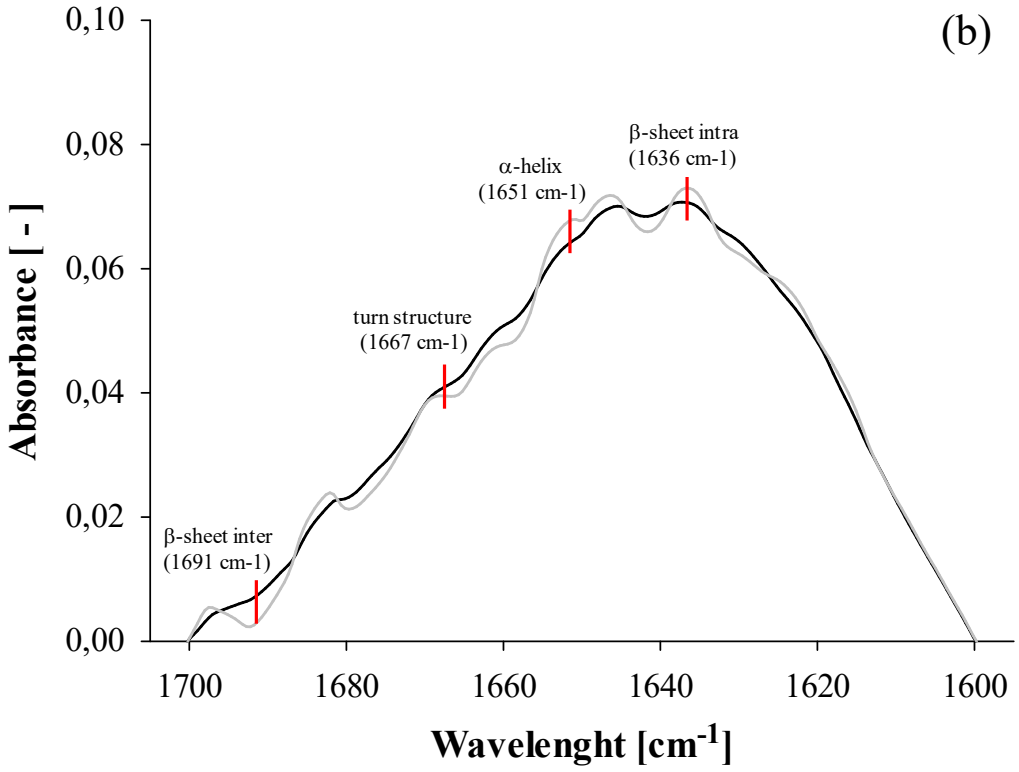
(b)
0,10
0,08
0,06
0,04
0,02
0,00
Absorbance [-]
β-sheet intra
(1636 cm-1)
α-helix
(1651 cm-1)
turn structure
(1667 cm-1)
β-sheet inter
(1691 cm-1)
1700
1680
1660
1640
1620
1600
Wavelenght [cm-1]

Figure 3

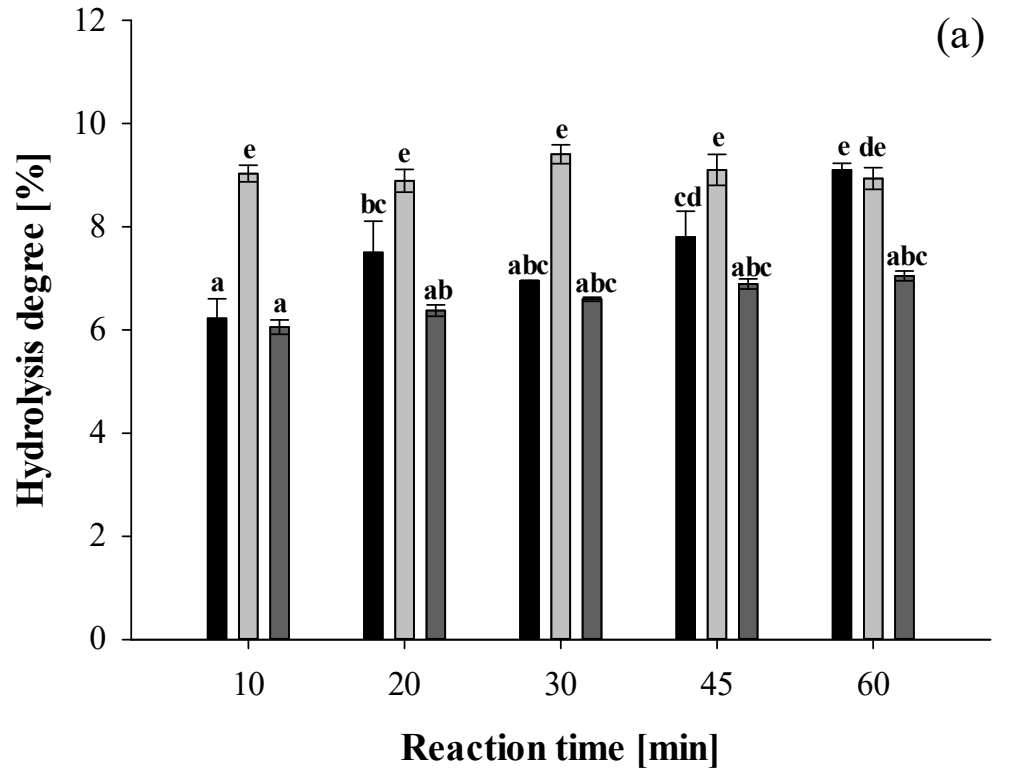
(a)
Hydrolysis degree [%]
12
10
8
6
4
2
0
a
e
a
bc
e
ab
abc
e
abc
cd
e
abc
e
de
abc
10
20
30
45
60
Reaction time [min]

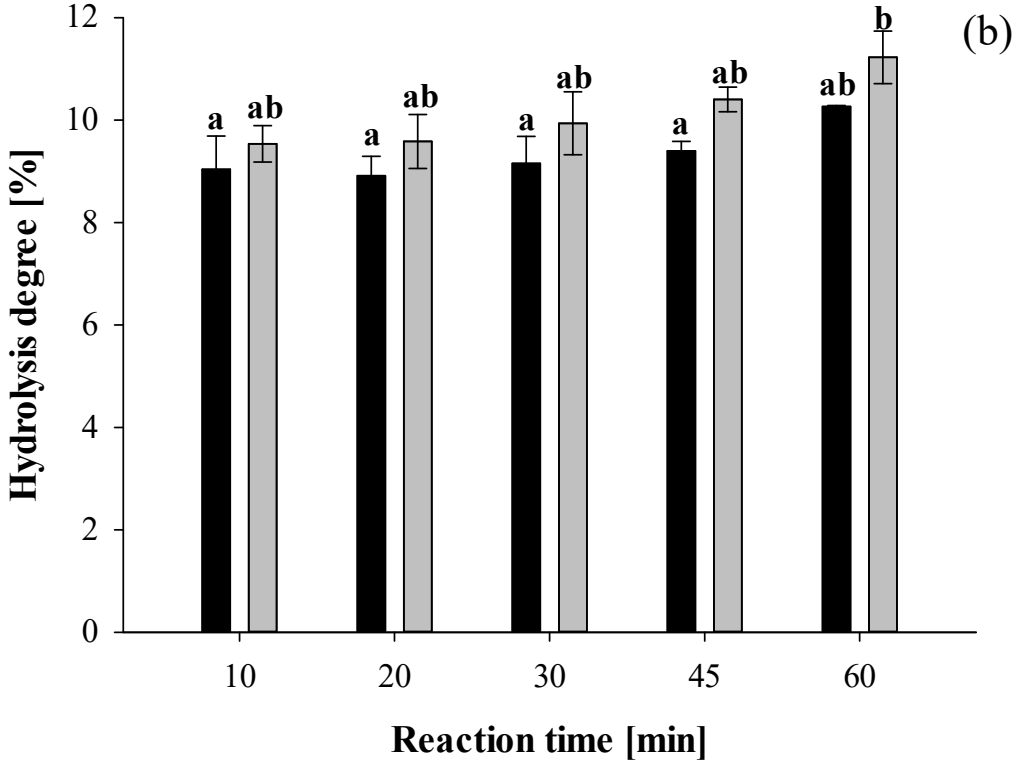
(b)
Hydrolysis degree [%]
12
10
8
6
4
2
0
a
ab
a
ab
a
ab
a
ab
ab
b
10
20
30
45
60
Reaction time [min]

Figure 4

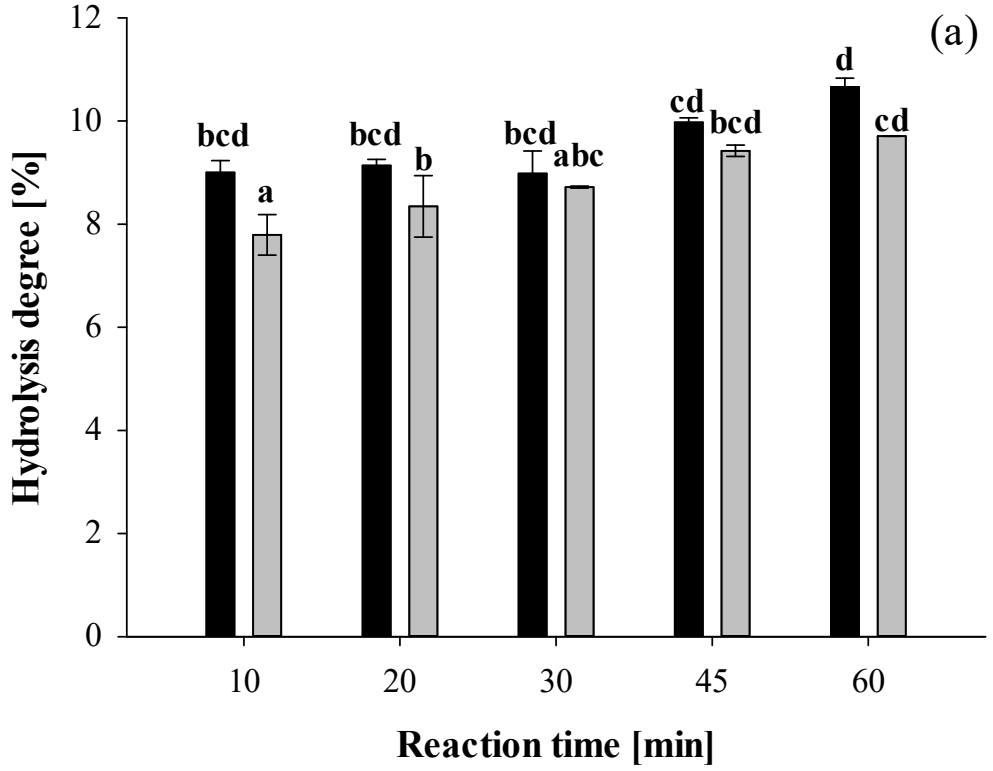
(a)
Hydrolysis degree [%]
0
2
4
6
8
10
12
bcd
a
bcd
b
bcd
abc
cd
bcd
d
cd
10
20
30
45
60
Reaction time [min]

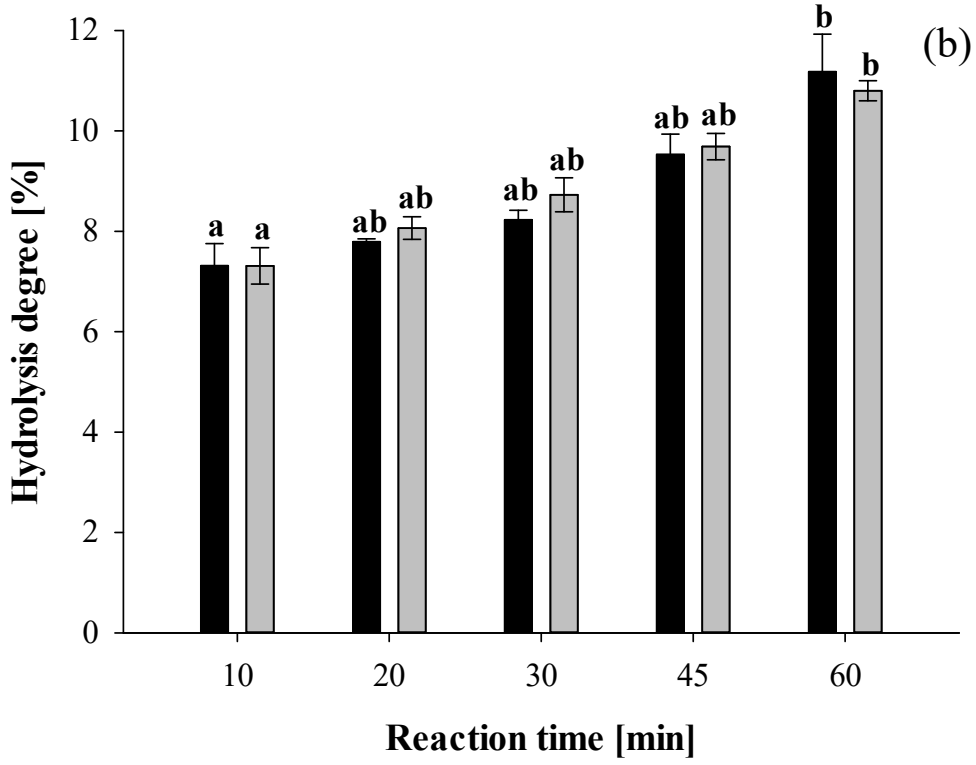
(b)
Hydrolysis degree [%]
0
2
4
6
8
10
12
a
a
ab
ab
ab
ab
ab
ab
b
b
10
20
30
45
60
Reaction time [min]

Figure 5

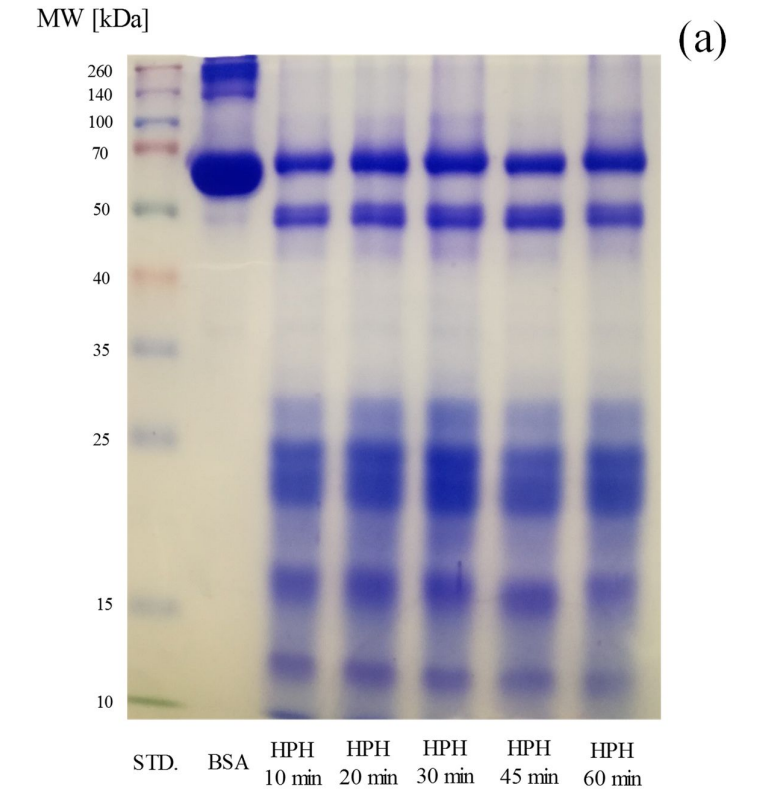
MW [kDa]
(a)
260
140
100
70
50
40
35
25
15
10
STD.
BSA
HPH 10 min
HPH 20 min
HPH 30 min
HPH 45 min
HPH 60 min

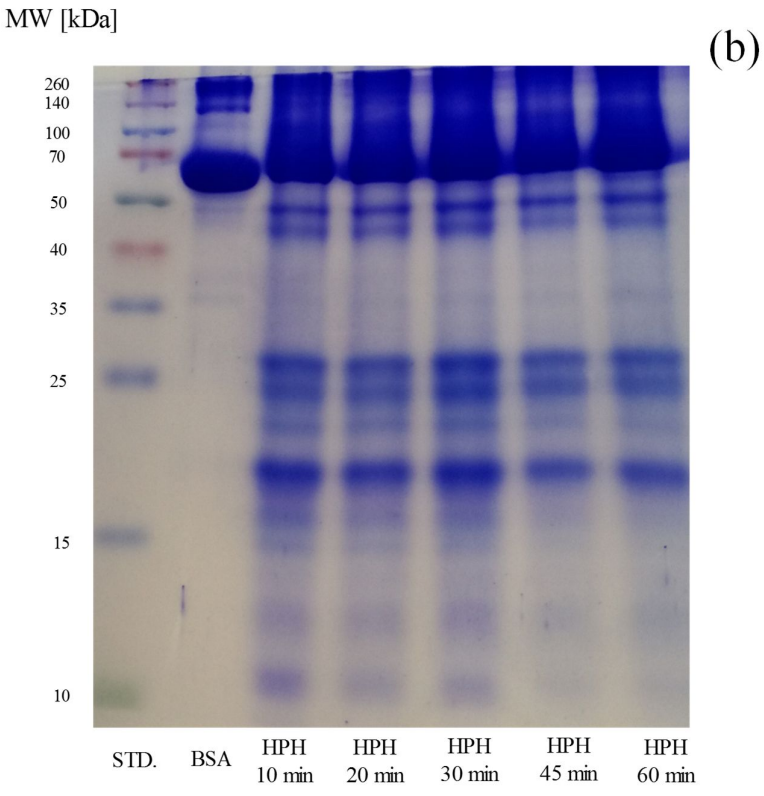
MW [kDa]
(b)
260
140
100
70
50
40
35
25
15
10
STD.
BSA
HPH 10 min
HPH 20 min
HPH 30 min
HPH 45 min
HPH 60 min

Figure 6

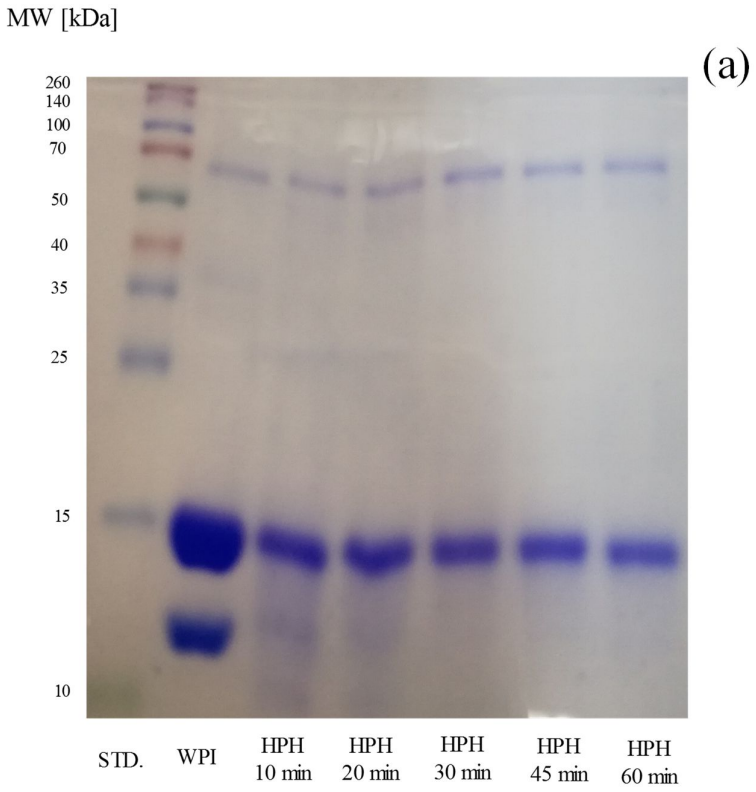
MW [kDa]
(a)
260
140
100
70
50
40
35
25
15
10
STD.
WPI
HPH 10 min
HPH 20 min
HPH 30 min
HPH 45 min
HPH 60 min

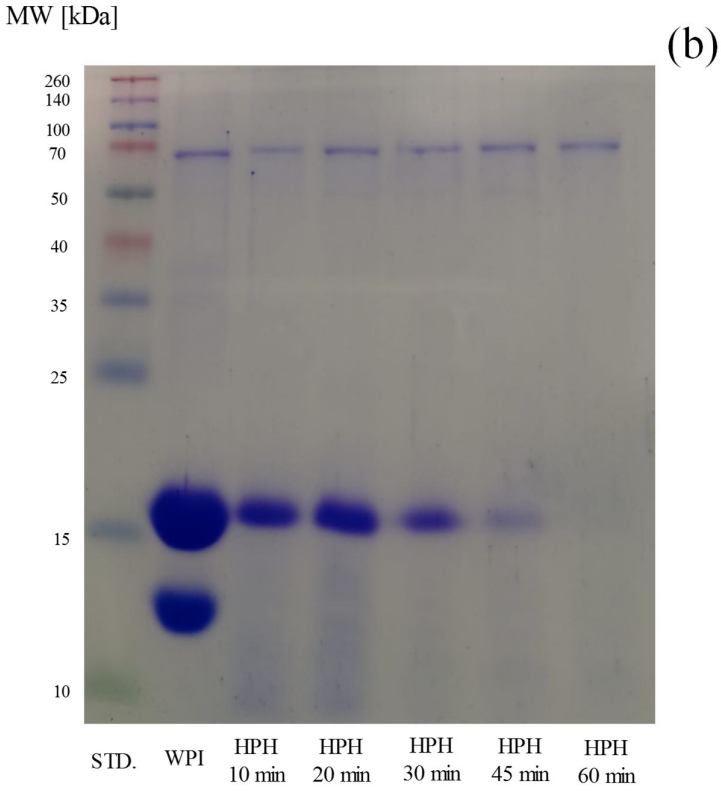
MW [kDa]
(b)
260
140
100
70
50
40
35
25
15
10
STD.
WPI
HPH 10 min
HPH 20 min
HPH 30 min
HPH 45 min
HPH 60 min